



## 1- ELECTRIC POWER SYSTEM WITH GOVERNOR DEADBAND

## 2- NONLINEARITY: MODELING AND CONTROL

3- IMAM R. M. EL-SEDAWI<sup>‡</sup>

## 4- ABSTRACT

This paper presents studies of the dynamic performance of a hydro-thermal power system under the effect of governor deadband nonlinearity. The describing function approach is utilized to handle the nonlinearity beside a linearized state space model for the rest of the system.

A new model is developed for the load frequency control problem of a two-area hydro-thermal power system comprised of thermal and hydro plant which differ widely in their characteristics. The optimal and decentralized control approaches are applied to control the behaviour of the system.

It is found that the principal effects of speed governor backlash nonlinearity produce more oscillations in area frequency deviation. Also, it is observed that the proposed control techniques improves system response and succeeded in stabilizing the system.

---

<sup>‡</sup> Lecturer, Dept. of Electric Machines & Power Engineering, Faculty of Engineering & Technology, University of Helwan, Helwan, Cairo, Egypt.

## INTRODUCTION

Power systems have been growing in size and complexity with increasing interconnection between systems. Interconnected operation ensures a more reliable power supply by sharing spinning reserve capacities during emergencies. In addition, it results in more economic operation when the diversity of the load in the different areas can be advantageously used. The problem of multiarea power systems based on linear models has received attentions of several authors [1-3].

In power systems the speed governor is a class of physical transmission elements which has the property of saturation, deadband and hysteresis. All governors have deadband, which are important for speed control under small disturbances because the deadbands affect the stability of the system [4,5].

Few work has been done concerning optimization of power systems taking the effect of governor nonlinearities. Reference [4] studied the effect of the governor deadband nonlinearity by considering a symmetrical two-area power system with reheat steam turbines. The dynamic behaviour of an electric power system is also investigated in [6] under the effect of speed governor rate and position limits. In the present work, we apply the proposed control algorithms for the design of power system controller to a two-area hydro-thermal with governor deadband nonlinearity which differ widely in their characteristics. The describing function approach is used to linearize the system and then to derive the model of a hydro-thermal power system. The proposed control technique is then applied to the developed model.

## DYNAMICAL MODEL FORMULATION WITH GOVERNOR DEADBAND

Hydro-electric power systems differ from steam electric power systems in that the relatively large inertia of the water used as a source of energy causes a considerably greater time lag in the response of the prime mover torque to a changing gate position. Also, for hydro turbine, there is an initial tendency for the torque to change in a direction opposite to that finally produced [5].

Governor deadband is defined as the total magnitude of a sustained speed change within which there is no change in valve position, or in other word it is a measure of its insensitivity to changes in system speed and is expressed in percent of rated speed, a typical value of which is 0.06% [4]. By representing the governor nonlinearities by the block shown in Fig.1. Following [4] and using the describing function analysis, the backlash nonlinearity introduces a time lag associated with the zero in the governor transfer function, as shown in Fig.1.

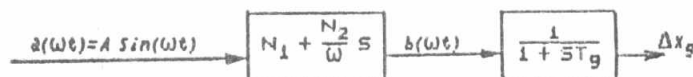


Fig.1. Backlash nonlinearity with speed governor model.

Then, the transfer function of the speed governor with backlash nonlinearity is given by [4].

$$\frac{X_g(s)}{a(s)} = \frac{(N_1 + \frac{N_2}{\omega} s)}{(1 + ST_g)} \quad (1)$$

where  $N_1$  and  $N_2$  are called the backlash coefficients and are given by:

$$N_1 = \frac{K}{\pi} \left\{ \frac{\pi}{2} - \sin^{-1} \left( \frac{2D}{A} - 1 \right) - \left( \frac{2D}{A} - 1 \right) \cos \left( \sin^{-1} \left( \frac{2D}{A} - 1 \right) \right) \right\} \quad (2)$$

$$N_2 = \frac{4DK}{\pi A} \left( \frac{D}{A} - 1 \right) \quad (3)$$

where  $A$  and  $\omega$  are the constant amplitude and frequency for the input sinusoidal waveform to the backlash, and  $K$  is the slope of hysteresis shown in Fig.2. A typical value of backlash is 0.06. However, by referring to the discussion in (4), it is found from Fig.3 that  $A/D=4$  will imply a backlash of approximately 0.05%.

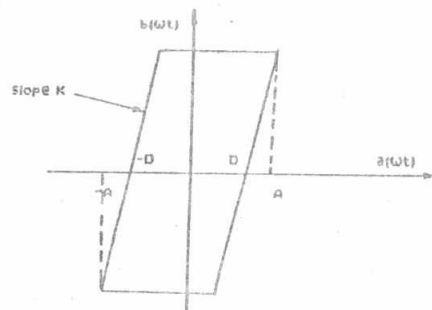


Fig.2. Governor backlash nonlinearity

This value of  $A/D$  for backlash of 0.05% is chosen for digital simulation in this work. Referring to Fig.3, the following backlash coefficients are obtained

$$\frac{N_1}{K} = 0.8$$

and

$$\frac{N_2}{K} = -0.2$$

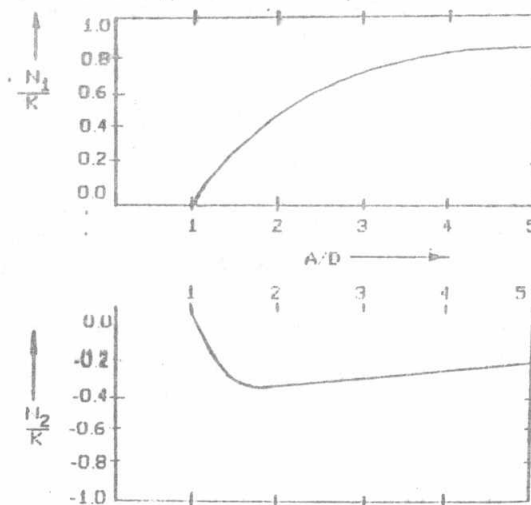


Fig.3. Coefficients of governor deadband against  $A/D$

The usual value of slope  $K$  of the curve in Fig.2 is 1, and the typical value of the load frequency control response indicates  $\omega = 2\pi f$  with  $f = 0.5\text{Hz}$  or  $\omega = \pi$ . Then from eq.(1)

$$\frac{X_g(s)}{a(s)} = \frac{(0.8 - \frac{0.2}{\pi} s)}{(1 + sT_g)} \quad (4)$$

The block diagram of a two-area hydro-thermal power system with governor deadband is shown in Fig.4. The thermal system (area 1) consists of non reheat turbines whereas the hydro-electric system (area 2) is considered to be equipped with a mechanical hydraulic governor.

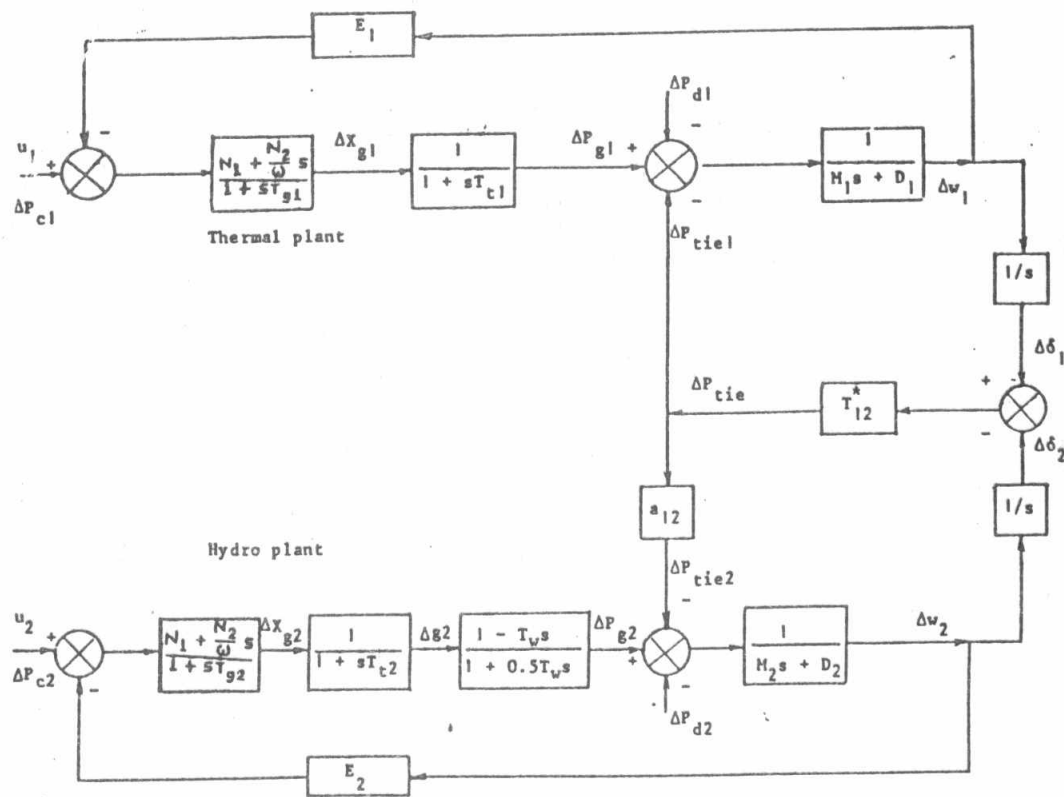


Fig.4 Block diagram of 2-area hydro-thermal power system with governor deadband nonlinearity.

The state vectors for the thermal and hydro areas respectively are defined as follows.

$$x_1^T = [\Delta\delta_1 \Delta\omega_1 \Delta P_{g1} \Delta X_{g1}] \quad (5)$$

$$x_2^T = [\Delta\delta_2 \Delta\omega_2 \Delta P_{g2} \Delta g_2 \Delta X_{g2}] \quad (6)$$

where  $\Delta\delta_i$  is the voltage angle deviation (rad) in area  $i$ ,  $i=1,2$ ;  $\Delta\omega_i$  is the angular frequency deviation ( $\text{rad}^{-1}$ ) in area  $i$ ,  $i=1,2$ ;  $\Delta P_{gi}$  is the deviation in mechanical

power (p.u. power) in area  $i$ ,  $i=1,2$ ;  $\Delta X_{gi}$  is the deviation in governor position (p.u. power) in area  $i$ ,  $i=1,2$ ;  $\Delta g_2$  is the deviation in gate position (p.u. power) in area 2. The speed changer positions  $\Delta P_{c1}$  and  $\Delta P_{c2}$  in p.u. power ( $u_1, u_2$ ) in area 1 and 2, are the two control inputs to the power system. The dynamic equations can be derived by the block diagram shown in Fig.4 as follow:

$$\Delta \delta_1 = \frac{1}{S} \Delta \omega_1 \quad (7)$$

$$\Delta \omega_1 = \frac{1}{M_1 S + D_1} [\Delta P_{g1} - \Delta P_{d1} - \Delta P_{tie\ 12}] \quad (8)$$

$$\Delta P_{g1} = \frac{1}{1 + T_{t1}} \Delta X_{g1} \quad (9)$$

$$\Delta X_{g1} = \frac{N_1 + \frac{N_2}{\omega} S}{1 + ST_{g1}} [\Delta P_{c1} - E_1 \Delta \omega_1] \quad (10)$$

$$\Delta \delta_2 = \frac{1}{S} \Delta \omega_2 \quad (11)$$

$$\Delta \omega_2 = \frac{1}{M_2 S + D_2} [\Delta P_{g2} - \Delta P_{d2} - \Delta P_{tie\ 21}] \quad (12)$$

$$\Delta P_{g2} = \frac{1 - T_w S}{1 + 0.5 T_w S} \Delta g_2 \quad (13)$$

$$\Delta g_2 = \frac{1}{1 + T_{t2}} \Delta X_{g2} \quad (14)$$

$$\Delta X_{g2} = \frac{N_1 + \frac{N_2}{\omega} S}{1 + ST_{g2}} [\Delta P_{c2} - E_2 \Delta \omega_2] \quad (15)$$

The expression of  $u_i$ ,  $i=1,2$  can be substituted from the following equations

$$u_i = \Delta P_{ci} = - \int ACE_i dt \quad (16)$$

where  $ACE_i$  is the area control error and is found by

$$\frac{d}{dt} \int ACE_i dt = \Delta P_{tie_i} + \beta_i \frac{\Delta \omega_i}{2\pi} \quad (17)$$

where  $\beta_i$  is the frequency bias parameter which determines the amount of interconnection during a disturbance in the neighbouring areas.

The system equations can easily be written in the compact form

$$\dot{x} = A x + B u + \Gamma d \quad (18)$$

where  $x$  is a (9x1) state vector,  $u$  is a (2x1) control vector, and  $d$  is a (2x1) disturbance vector. The state distribution matrix  $A$  (9x9), the input matrix  $B$  (9x2) and the disturbance matrix  $\Gamma$  (9x2) in this case, have the following structure:

$$\begin{aligned}
 A = & \begin{bmatrix}
 0 & 1 & 0 & 0 & 0 & 0 & 0 & 0 & 0 \\
 \frac{-T_{12}^*}{M_1} & \frac{-D_1}{M_1} & \frac{1}{M_1} & 0 & \frac{T_{12}^*}{M_1} & 0 & 0 & 0 & 0 \\
 0 & 0 & \frac{-1}{T_{t1}} & \frac{1}{T_{t1}} & 0 & 0 & 0 & 0 & 0 \\
 Y_1 & Z_1 & \frac{-N_2 E_1}{\omega T_{g1} M_1} & \frac{-1}{T_{g1}} & Y_1 & 0 & 0 & 0 & 0 \\
 0 & 0 & 0 & 0 & 0 & 1 & 0 & 0 & 0 \\
 \frac{-a_{12} T_{12}^*}{M_2} & 0 & 0 & 0 & \frac{a_{12} T_{12}^*}{M_2} & \frac{-D_2}{M_2} & \frac{1}{M_2} & 0 & 0 \\
 0 & 0 & 0 & 0 & 0 & 0 & \frac{-2}{T_w} & \left( \frac{2}{T_w} + \frac{2}{T_{t2}} \right) & \frac{-2}{T_{t2}} \\
 0 & 0 & 0 & 0 & 0 & 0 & 0 & \frac{-1}{T_{t2}} & \frac{1}{T_{t2}} \\
 Y_2 & 0 & 0 & 0 & Y_2 & Z_2 & \frac{-N_2 E_2}{\omega T_{g2} M_2} & 0 & \frac{-1}{T_{g2}}
 \end{bmatrix} ; \\
 B^T = & \begin{bmatrix}
 0 & 0 & 0 & \frac{N_1}{T_{g1}} & 0 & 0 & 0 & 0 & 0 \\
 0 & 0 & 0 & 0 & 0 & 0 & 0 & 0 & \frac{N_1}{T_{g2}}
 \end{bmatrix} ; \\
 \Gamma^T = & \begin{bmatrix}
 0 & \frac{-1}{M_1} & 0 & \frac{N_2 E_1}{\omega T_{g1} M_1} & 0 & 0 & 0 & 0 & 0 \\
 0 & 0 & 0 & 0 & 0 & \frac{-1}{M_2} & 0 & 0 & \frac{N_2 E_2}{\omega T_{g2} M_2}
 \end{bmatrix} \quad (19)
 \end{aligned}$$

where for area  $i$  ( $i=1,2$ ),  $E_i$  is the area frequency response characteristic;  $M_i$  is the effective rotary inertia (p.u. MWS<sup>2</sup>);  $D_i$  is the load frequency constant (p.u. MWS rad<sup>-1</sup>);  $T_{ti}$  is the turbine time constant (S);  $T_{gi}$  is the speed governor time constant (S);  $T_w$  is the water starting time constant in seconds (hydro area);  $T_{12}^*$  is the tie line power flow constant at operating conditions;  $a_{12}$  is constant;

$$Y_1 = \frac{N_2 T_{12}^*}{\omega T_{g1}} \left[ -1 + \frac{E_1}{M_1} \right]; \quad (20)$$

$$Z_1 = \frac{1}{\omega T_{g1} M_1} \left[ N_2 M_1 \beta_1 - N_1 E_1 M_1 \omega + N_2 E_1 D_1 \right]; \quad (21)$$

$$Y_2 = \frac{a_{12} N_2 T_{12}^*}{\omega T_{g2}} \left[ -1 + \frac{E_2}{M_2} \right]; \text{ and} \quad (22)$$

$$Z_2 = \frac{1}{\omega^T g_2^T M_2} [N_2 M_2 \beta_2 - N_1 E_2 M_2 \omega + N_2 E_2 D_2] \quad (23)$$

The transient response requirements of the system necessitates the minimization of the function

$$\min J = \int_0^{\infty} (\Delta \delta_1^2 + \Delta \omega_1^2 + \Delta \delta_2^2 + \Delta \omega_2^2 + u_1^2 + u_2^2) dt \quad (24)$$

The objective of the next section is to design controller that generates speed changer command signals,  $\Delta P_{c1}$  and  $\Delta P_{c2}$ , which minimize the function (24) subject to the system dynamic constraint given by (18).

### OPTIMIZATION SCHEME

The dynamic of the interconnected power system may be described as an interconnection of  $N$  subsystems represented by

$$\dot{x}_i = A_i x_i + B_i u_i + \sum_{j=1}^N H_{ij} x_j, \quad i=1,2,\dots,N \quad (25)$$

Associated with each subsystem is a performance index  $J_i$  of the form

$$J_i = 1/2 \int_0^{\infty} (x_i^T Q_i x_i + u_i^T R_i u_i) dt \quad (26)$$

where  $x_i$  is the  $n_i$ -dimensional state vector of the  $i$ th subsystem,  $u_i$  is the  $m_i$ -dimensional control vector,  $Q_i$  is at least a positive semi-definite matrix, and  $R_i$  is a positive matrix. Also

$$A_i = \text{block diag. } [A_1, A_2, \dots, A_N],$$

$$B_i = \text{block diag. } [B_1, B_2, \dots, B_N];$$

and  $H_{ij}$  is the interconnection matrix. The problem is how to find decentralized controller  $u_i$  of the form

$$u_i = -F_i x_i, \quad i = 1,2,\dots,N \quad (27)$$

which minimizes  $J_i$ . Consider the isolated decoupled subsystem in which the interaction vectors are assumed to be zero

$$\dot{x}_i = A_i x_i + B_i u_i, \quad i = 1,2,\dots,N \quad (28)$$

each of subsystems described by (28) can minimize  $J_i$ , when the control vectors are given by

$$u_i = -R_i^{-1} B_i^T P_i x_i, \quad i = 1,2,\dots,N \quad (29)$$

where  $P_i$  is symmetric positive definite solution of matrix Riccati equation

$$A_i^T P_i + P_i A_i - P_i (B_i R_i^{-1} B_i^T) P_i + Q_i = 0 \quad (30)$$

Then the closed loop decoupled subsystems are given by

$$\dot{x}_i = (A_i - B_i R_i^{-1} B_i^T P_i) x_i, \quad i = 1,2,\dots,N \quad (31)$$

using the control  $u_i$  of (29), the system (25) is described by

$$\dot{x}_i = (A_i - B_i R_i^{-1} B_i^T P_i) x_i + \sum_{j=1}^N H_{ij} x_j, \quad i = 1, 2, \dots, N \quad (32)$$

We can observe that this decentralized scheme is developed to improve the performance of the system. In the next section, the decentralized technique is applied to the power system model.

### SIMULATION RESULTS

The following numerical data have been used by [1,6] for load frequency control studies of the two-area hydro-thermal power system:

$M_1 = 0.167$  p.u.;  $D_1 = 0.00833$  p.u.;  $E_1 = 0.416$  p.u.;  $T_{g1} = 0.2$  Sec;  $T_{t1} = 0.3$  Sec;  $M_2 = 0.03$  p.u.;  $D_2 = 0.008$  p.u.;  $E_2 = 0.013$  p.u.;  $T_{g2} = 1.2$  Sec;  $T_{t2} = 0.5$  Sec;  $T_w = 0.5$  Sec;  $r_{12}^* = 0.02701$ ;  $a_{12} = -1$ ;  $\beta_1 = \beta_2 = 0.425$ . Furthermore, the speed governor backlash coefficients are given as in section 2.

#### Case study 1:

We consider the uncontrolled power system; i.e.  $u_1 = u_2 = 0$ , with and without governor deadband nonlinearity. The system dynamic responses are presented in Figs.5-8. The principal effects of governor deadband nonlinearity in this case is to produce more oscillations and instability has been observed.

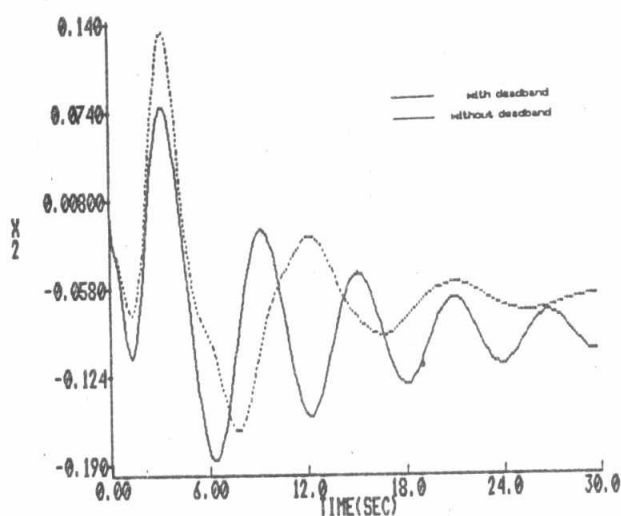


Fig. 5

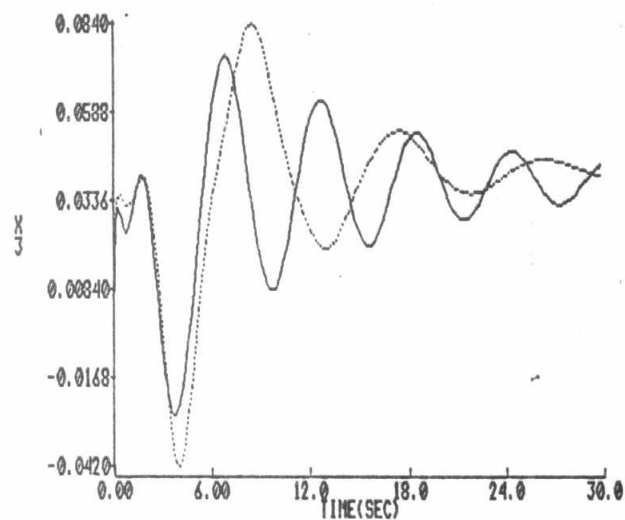


Fig. 6

#### Case Study 2:

Following the decentralized control optimization technique as in section 3, and for the sake of comparison, the closed loop system has been simulated in each of the following cases:

- The complete decentralized control (decoupled)
- Decentralized control with interaction (coupled)



## c) Centralized optimal control

The simulation results are shown in Figs. 9-12 to illustrate the effect of governor-deadband nonlinearity. It is observed that the increased oscillations in the system response as a whole in the area frequency deviations and the stability of the system is not threatened by using the control techniques adopted in this paper.

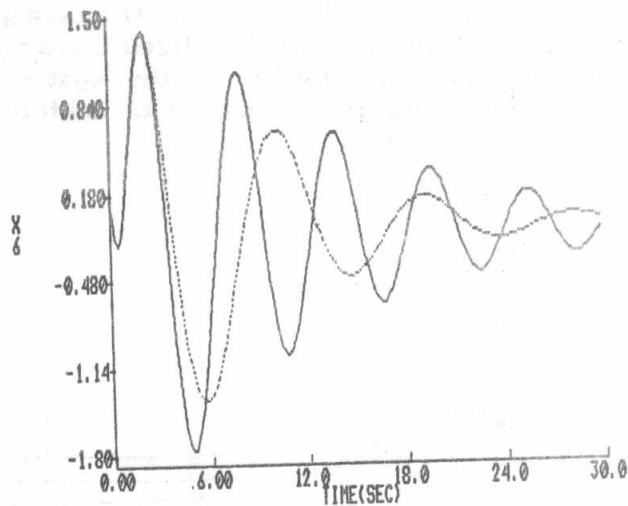


Fig. 7

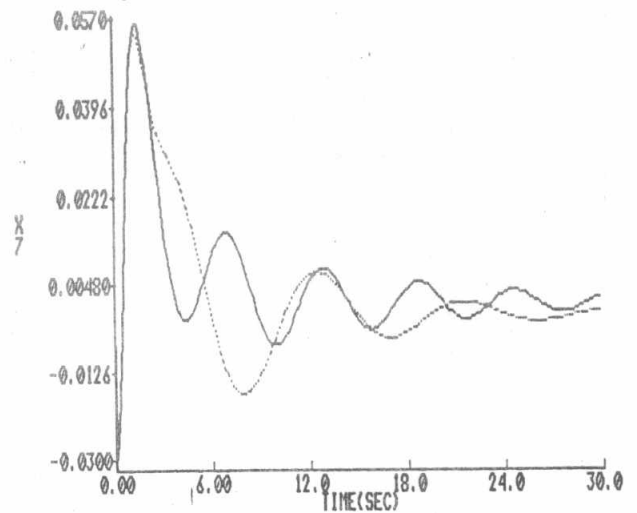


Fig. 8

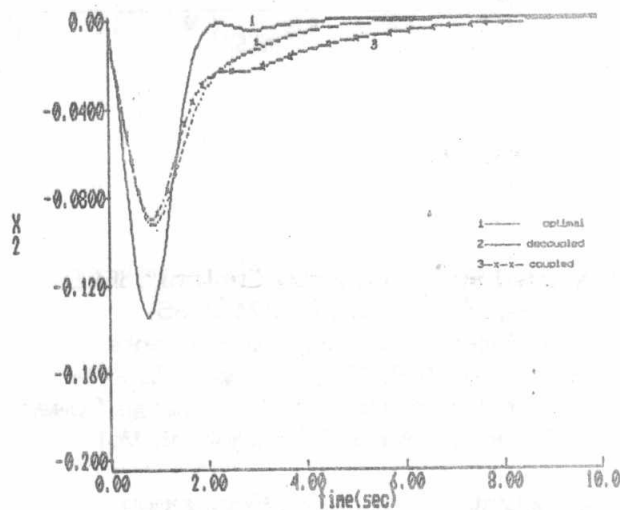


Fig. 9

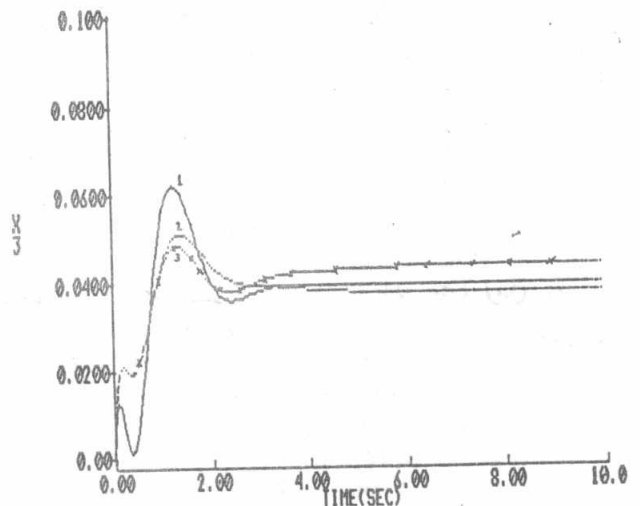


Fig. 10

It is found that the proposed decentralized controller give satisfactory results for this system having comparatively strong interaction among its areas. The results indicate that zero steady state errors in frequency can be achieved.

Moreover, the settling time is reduced ( about 6-8 sec ) better than other conventional controllers [4] ( about 120 sec ).

### CONCLUSION

A new model for a hydro-thermal power system with governor deadband nonlinearity has been developed in this paper. The decentralized control technique has been applied to the two-area model. It is found that the principal effects of speed governor backlash nonlinearity produce more oscillations in area frequency deviation. Also, it is observed that the decentralized and centralized control techniques improves system response and succeeded in stabilizing the system. The results indicates that the proposed methods can simplify the design of control system for large-scale power plant.

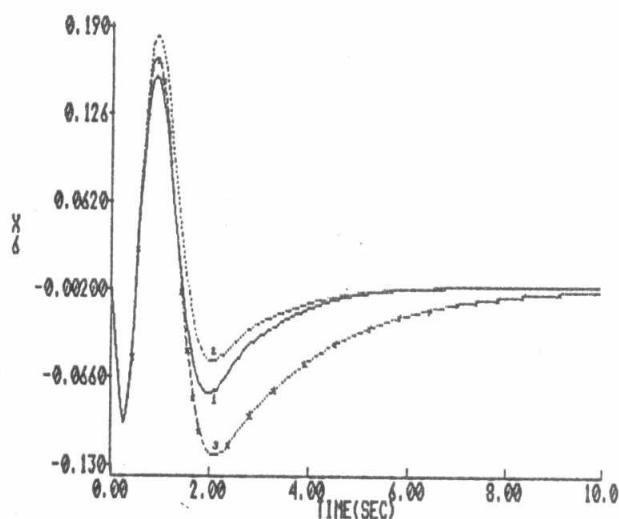


Fig. 11

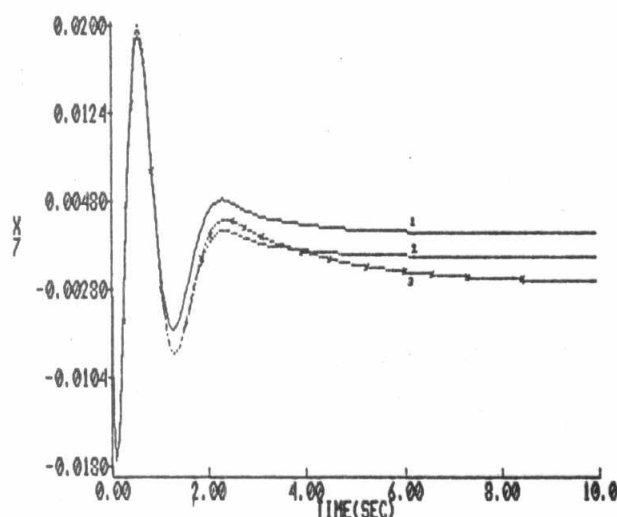


Fig. 12

### REFERENCES

- 1- Calovic, M. "Linear Regulator Design for a Load and Frequency Control", IEEE Trans. in Power Apparatus and Systems, Vol: PAS-91, 1971, pp:2271-2285.
- 2- Miniesy, S.M.; Bohn, E.V. "Two-Level Control of Interconnected Power Plants", IEEE Trans. on Power Apparatus and Systems, Vol: PAS-90, 1971, pp:2422-2448.
- 3- Davison, E.J.; Tripathi, N.K. "The Optimal Decentralized Control of a Large Power System: Load and Frequency Control", IEEE Trans. on Automatic Control, Vol: AC- 23, No.2, April 1978, pp:312-325.
- 4-Tripathy, S.C.; Hope, G.S.; Malik, O.P. "Optimization of Load-Frequency Control Parameters for Power Systems with Reheat Steam Turbines and Governor Deadband Nonlinearity", IEE Proc., Vol:129, Pt:C, No.1, Jan. 1982, pp:10-16.
- 5-Kirchmayer, L.K. "Economic Control of Interconnected Systems", John Wiley & Sons, New York, 1959.
- 6-El-Sedawi, I.R.M.; Roberts, P.D.; Gopal, M. "Multilevel Optimization of a Hydro-Thermal Interconnected Power System", Int. J. Sys. Sci., 1989, Vol:20, No.8, pp:1467-1482.